

Pancreatic Cancer Segmentation and Classification in CT Imaging using Antlion Optimization and Deep Learning Mechanism

Radhia Khdhir¹, Aymen Belghith², Salwa Othmen³

Department of Computer Science-College of Science and Arts in Qurayyat, Jouf University, Saudi Arabia¹
Computer Science Department-College of Informatics and Computing, Saudi Electronic University, Saudi Arabia²
Computers and Information Technology Department, College of Science and Arts, Saudi Arabia³

Abstract—Pancreatic cancer, a fatal type of cancer, has a very poor prognosis. To monitor, forecast, and categorise cancer presence, automated pancreatic cancer segmentation and classification utilising Computer-Aided Diagnostic (CAD) model can be used. Furthermore, deep learning algorithms can provide in-depth diagnostic knowledge and precise image analysis for therapeutic usage. In this context, our study aims to develop an Antlion Optimization-Convolutional Neural Network-Gated Recurrent Unit (ALO-CNN-GRU) model for pancreatic tumor segmentation and classification based on deep learning and CT scans. The ALO-CNN-GRU technique's objective is to segment and categorize the presence of cancer tissues. This technique consists of pre-processing, segmentation and feature extraction and classification phases. The images go through a pre-processing stage to reduce noise from the dataset that was obtained. A hybrid Gaussian and median filter is applied for the pre-processing phase. To identify the pancreatic area that is affected, the segmentation is processed utilizing the Antlion optimization method. Then, the categorization of pancreatic cancer as benign or malignant is done by employing the classifiers of the Convolutional neural network and Gated Recurrent Unit networks. The suggested model offers improved precision and a better rate of pancreatic cancer diagnosis with an accuracy of 99.92%.

Keywords—Pancreatic cancer; Antlion optimization; deep learning; convolutional neural network

I. INTRODUCTION

The pancreas is a vital organ in the human body that secretes both internally and externally and is prone to several illnesses. Deeper within the belly, the pancreas is a glandular organ [1]. It is made up of the endocrine and exocrine tissues, which, separately, are essential to digestion and glucose metabolism. Endocrine and exocrine pancreatic illnesses are divided into categories based on the tissue most frequently impacted by pathologies. Chronic pancreatitis, pancreatic cancer, and acute pancreatitis are exocrine pancreas diseases. There is an increasing realization that these three conditions exist on some kind of continuous sequence [2]. Pancreatic endocrine malfunction, a key factor connecting the various kinds of diabetes mellitus, characterizes disorders of the endocrine pancreas. Diabetes of the exocrine pancreas, type 1 DM and type 2 DM, make up the bulk of the spectrum in terms of prevalence in adults [3]. There are other forms of DM as well. Consequently, disorders of the endocrine and exocrine

pancreas place enormous socioeconomic and health costs on people across the world.

Pancreatic cancer has a relatively high mortality rate that closely resembles its incidence rates. The fourth most frequent cause of cancer mortality and the twelfth most frequent cause of cancer overall is pancreatic cancer [4]. 62,210 new cases of pancreatic cancer are anticipated to be discovered in the USA in 2022 with a percentage of 3.2% of all cancer cases. Pancreatic cancer patients typically have vague symptoms, such as loss of weight and abdominal discomfort, which can delay detection. Usually, pancreatic cancer patients experience no symptoms up to an established stage of the illness. A standardized approach for monitoring individuals who are at risk of pancreatic cancer does not exist, yet [5]. Pancreatic intraepithelial neoplasias, which are tiny, non-invasive epidermal proliferations inside the pancreatic ducts, are the primary causes of most pancreatic malignancies. The exceedingly dismal outcome for pancreatic cancer is underlined by the strong correlation between disease occurrence and death. In USA, the five-year survival rate for those with pancreatic cancer is still as low as 7%. The terminal stage at which the majority individuals are identified is among the causes of the lower survival rate and is arguably the most significant one. Prior to the illness progressing to an advanced phase, the majority of pancreatic cancer patients have no symptoms [6].

Numerous techniques based on deep learning and machine learning have recently been proposed to identify pancreatic cancer because of the invention of Computer-Aided Diagnosis (CAD). Accurate segmentation of the pancreatic and reliable categorization are often necessary for an automated and elevated pancreas cancer diagnostic model [7]. In everyday practice, pancreatic disorders are diagnosed and monitored using cutting-edge cross-sectional imaging techniques such as computed tomography, magnetic resonance cholangiopancreatography, magnetic resonance imaging, and endoscopic ultrasonography (EUS). Through these techniques, the complete pancreas may be seen in connection to the adjacent anatomy [8]. The most frequently employed imaging technique for the first assessment of suspicious pancreatic cancer is computed tomography. It is chosen over Magnetic Resonance Imaging (MRI) as the initial line modalities because it is less expensive and more widely accessible than MRI. A more accurate assessment of the pancreatic

parenchyma and calcifications can be made using computed tomography. Structural information may be obtained from Computerized Tomography (CT) scans. The preferred imaging technique for diagnosing pancreatic illness nowadays is contrast-enhanced CT, which may also have the best standard specifications rates for pancreatic cancer. In various fields, the segmentation of the pancreas in CT images can help clinical processes, such as pancreatic cancer detection, treatment, and surgical support [9]. Therefore, it is worthwhile to investigate a reliable, accurate, and automated segmentation approach for the pancreas.

In abdominal computed tomography images, segmenting organs including the liver, spleen, and pancreas is essential for computer-aided diagnosis, quantitative and qualitative studies, and surgical support. In CAD systems that do quantitative image analysis of people with diabetes or pancreatic diagnostic tools, pancreas segmentation in particular is a crucial component. Because of its size, shape, and position in the abdomen on computed tomography scans, the pancreas is extremely difficult to segment [10]. In the area of organs segmentation, the network architectures of UNet, SegNet and FCN are especially well-liked, and all these techniques have been successfully used in the segmentation of big organs, such as the heart, kidneys, and lungs. The segmentation of minor organs might still use different approach. Particularly challenging in terms of form learning are the extremely intricate anatomical components of the pancreatic. Second, there is a dearth of annotated medical imaging data [11]. As a result, the segmentation is unable to achieve a high level of precision. Additionally, the pancreas' location in the abdominal wall differs from patient to patient, and the border contrast is influenced by the amount of visceral fat that surrounds the pancreas. These additional elements are combined to make pancreatic segmentation difficult and susceptible to both over and under-segmentation. To address these issues, we aim to develop a powerful pancreatic segmentation approach that will improve the precision and robustness of pancreatic segmentation.

Because the pancreas is more varied in size and shape than other organs and is challenging to categorize with neighboring organs, segmenting it is a challenging process. The manual segmentation of the pancreas by radiologists requires a lot of time and effort. Additionally, there are variations in the manual results produced by radiologists. Even though advanced machine learning technology, techniques were put forth to separate the pancreas after extracting specific properties utilizing prior information [12]. Numerous deep learning-based studies have been recently completed as hardware efficiency and deep learning technologies have advanced. The results have outperformed earlier approaches in a variety of applications. The convolutional neural network, one of several deep learning methods, performs well for the segmentation and classification challenge and may be efficiently used to segment the pancreas [13].

The research's main contributions are as follows:

- A significant number of patients' CT images are first gathered, and the CT datasets are analysed in the system.

- Furthermore, the recovered CT pancreatic images contain unwanted noises, which are filtered utilizing an advanced Gaussian and median filter.
- An upgraded Antlion Optimization model has been used for the segmentation process.
- Gray Level Co-occurrence Matrix was used for feature extraction.
- The ALO-CNN-GRU classifies the affected regions as benign and malignant.
- The efficacy of the suggested technique is demonstrated by validating its performance and comparing it to current methodologies.

The paper is structured as follows. Several related works are covered in Section II. The suggested ALO-CNN-GRU architectures are explored in depth in Section III. In Section IV, experiment findings are shown, evaluated, and a thorough assessment of the suggested strategy in comparison to current best practices is made. In Section V, the final portion of the document, the work is concluded.

II. RELATED WORKS

In order to improve the segmentation of pancreatic cancer, Jun Li et al. suggested a dual meta-learning approach based on idle data [14]. For clinical treatment and detection of pancreatic cancer, automated segmentation is essential. The segmentation performance is however constrained by the tiny size and hardly perceptible borders. Researchers gather pancreatic cancer unused multi-parametric Magnetic resonance imaging from numerous researches to build a significantly larger dataset for improving the Computed tomography pancreatic cancer segmentation in order to resolve the issue brought on by the small-scale dataset. So, for pancreatic cancer, researchers suggest a deep learning segmentation technique with a dual meta-learning structure. Elevated characteristics become more discriminatory as a result of its ability to combine salient information from CT images. In order to flawlessly satisfy the gaps in visual appeal as well as provide rich intermediate depictions for the ensuing meta-learning scheme, the arbitrary transitional methods between CT and MRIs are generated. Researchers then use prototype meta-learning based on transitional modes to identify and transmit similarities. The distraction caused by internal variations is finally reduced by using a meta-optimizer to flexibly understand the relevant characteristics inside CT data. The suggested approach is a robust pancreatic cancer segmentation approach that is simple to implement into existing segmentation networks and has promise as a viable model for addressing the problems of data scarcity with idle data but its accuracy is very low when compared to the other existing models.

A Deep Learning-Enabled Automated Medical Decision-Making System for Pancreatic Tumor Diagnosis on Computed Tomography was proposed by Thavavel Vaiyapuri et al. [15]. The computer-aided diagnostic model can automatically identify and categorize pancreatic cancers. Deep learning and Machine learning models that have lately been created can be utilized to automatically and quickly diagnose pancreatic

cancer. The study introduces an innovative deep-learning-enabled medical decision-making system for classifying pancreatic tumors from CT scans. The IDLDMS-PTC technique's primary goal is to assess the CT images for the presence of pancreatic tumors. An emperor's penguin optimizer with multilayer thresholding approach is derived using the IDLDMS-PTC model for segmenting pancreatic tumors. Furthermore, the MobileNet algorithm is used as an optimum feature extractor for classifying pancreatic tumors. The multileader optimization approach is employed to alter the bias and weight parameters of the AE approach in the best possible way. The innovative features are demonstrated by the EPO algorithm's design for selecting the best threshold and by the MLO algorithm's design for parameter adjustment. Numerous simulations were run on data sets, and the results showed that the IDLDMS-PTC model performed well compared to other techniques but the model still needs improvements.

The Anatomy-Aware Transformers were addressed by Yingda Xia et al. for the efficient pancreatic cancer screening [16]. The most fatal malignancy, pancreatic cancer is quite infrequent. It is not advised to screen the entire asymptomatic populace because to the possibility that a sizable proportion of false positive people may have unneeded imaging tests, considerably increasing health care expenditures with no discernible patient benefits. In the study, researchers explore the viability of detecting respectable pancreatic masses utilizing a single-phase non-contrast CT scan and classifying the detected masses as pancreatic ductal adenocarcinoma, other anomalies, or healthy pancreas. The majority of the time, regular radiologist or perhaps even pancreatic experts perform the duty ineffectively. Researchers suggest a novel deep classification method with an anatomy transformer employing pathology verified mass kinds and transfer of knowledge from contrast-enhanced Computed tomography to non-contrast Computerized Tomography as supervision. The research identifies a possible new instrument with considerably higher accuracy and reduced computational risk and cost for widespread pancreatic screening and treatment. However, the proposed instrument is not able to analyze vast amounts of data.

Xiaoyu Yang et al. used Interpolation neural network with local linear embedding for cancer progression segmentation [17]. The thick Computed tomography with its low resolution and wide spacing increases the risk of misinterpretation and makes it extremely difficult to automatically separate organs and tumors. Because of the technology limitations, particularly in automated pancreatic tumor segmentation, there is poor consistency among segments of the 3D CT image containing few tumors per image. In addition, tumor characteristics, such as size, form, localization, and severity, vary greatly between instances. The segmentation process is very unclear due to the hazy borders of tiny tumors. Researchers integrate the LLE-based interpolation neural network into the pancreatic tumor segmentation challenge in an effort to address these issues, which primarily incorporates the following enhancements. To represent the connection between nearby segments and the interpolated segment, researchers use local linear embedding. It adjusts the organ's

geometric transition between segments. The LLE module and neural network work together to greatly improve image quality, resulting in more consistent and sharper images being produced for each sequence. The system utilizes a multiscale cascading technique to lessen the impact of sudden changes in tumor size on segmentation outcomes. Furthermore, to improve accuracy, the mechanism must be improved.

Vahid Asadpour et al. analyzed pancreatic cancer tumors in Computed tomography images using a patch-based multi-resolution convolutional neural network. In the article, researchers suggested a cascaded framework for extracting the volumetric form of the tumor and pancreas in adenocarcinoma patients. The method combines an elastic atlas that can fit on 3D volumetric shape retrieved from Computed tomography slices, a convolutional network with multiple forward pathways to recognize the fragments of images with particles to good resolutions using a multi-resolution structure. Geometrical characteristics that were altered both globally and per organ were employed to value the atlas organs. A multiresolution CNN was utilized for the categorization of image patches. By using an edge detection technique, the pancreas and tumor were finally segmented. The completely cascaded technique that has been developed outperformed all other methods in comparison. However, it takes a lengthy time to analyze data compared to other approaches [18].

The Preoperative Estimation of Pancreatic Survival Rates and Operational Margins utilizing Contrast-Enhanced CT Imaging were described by Jiawen Yao et al. [19]. One of the deadliest fatal malignancies, pancreatic ductal adenocarcinoma, has a poor prognosis. For individuals who are qualified for first treatment of PDAC, surgery continues to provide the highest chance of a possible cure. Nevertheless, even among resected individuals who were at the similar stage and got identical therapies, results might differ dramatically. In the study, researchers introduce a unique deep neural network called 3D CE-ConvLSTM, which can extract the tumor regression characteristics or features from CE-CT imaging techniques, for the survival prediction of PDAC victims. Researchers describe a multi-task CNN that can predict margins and outcomes, and which gains from understanding variables associated with tumor resection margins to enhance survival prediction. Comparing the suggested framework to current cutting-edge techniques to survival analysis, prediction performances must be improved.

An Effective Deep Learning-Based Pancreatic Cancer and Non cancer Categorization Model Utilizing CT scans were proposed by Maha M. Althobaiti et al. [20]. The prognosis for pancreatic tumors, which are a fatal kind of tumor, is quite dismal. To monitor, anticipate, and categorize the presence of pancreatic tumors, an automated pancreatic tumor categorization employing a computer-aided diagnostic model is required. Artificial intelligence can provide in-depth diagnostic knowledge and precise picture interpretations during treatment. The work develops an ODL-PTNTC model for optimum deep learning-based pancreatic tumor and nontumor categorization utilizing CT images. The ODL-PTNTC method's objective is to identify and categorize pancreatic tumors and non-tumors. Adaptive window filtering

is a method included in the suggested ODL-PTNTC approach to eliminate noise. Additionally, the image segmentation procedure uses the Sailfish Optimizer based Kapur's Thresholding approach. A collection of feature vectors is also produced through feature extraction utilizing the Capsule Network. For categorization reasons, Political Optimizer with CFNN is also used. The performance of the classifier of the ODL-PTNTC approach can be enhanced by DL-based segmentation methods.

III. PROPOSED METHODOLOGY

In the beginning, pancreatic cancer images from Computerized Tomography (CT) are gathered. After that, the images are employed for testing and training. Pre-processing of pancreas-dependent CT images involves the removal of extraneous noise using a combined Gaussian and median filter. In this study, the nodules associated with pancreatic cancer are found and segmented using the Antlion optimization method. The Grey Level Co-occurrence Matrix is then used to extract the features. The suggested ALO-CNN-GRU method is utilized to categorize the aggressiveness of pancreatic cancer nodules. Fig. 1 represents the proposed method's framework.

A. Dataset Description

From the General Hospital of the Shenyang Military Area Command, 80 patients' CT data were analyzed. A total of 1700 images in Digital form are included in every pair of CT imaging sequence. Each CT picture is 512 x 512 pixels in resolution. There are 40 patients who have pancreatic cancer, while the others are well. Both malignant and benign pancreatic cancer images can also be found in the CT imaging. Three nuclear medicine specialists choose the descriptions for the images. Researchers perform segmentation tests using the NIH pancreatic segmentation dataset, which comprises 82 abdominal contrast-enhanced 3-Dimensional CT images, to fairly compare our segmentation approach to others. The surface pancreatic segmentation masks have indeed been submitted by a med student and have been reviewed by a radiologist. 1782 CT data are present, of which 863 serve as the training datasets and 919 serve as the testing datasets.

B. Pre-Processing

The initial stage in the identification of pancreatic cancer is pre-processing. It is employed to remove extraneous data and fill in dataset shortages. The evaluation of the sample images is slowed down by unrelated and unexpected sounds that affect the computed tomography images. The speckle noises that are brought on by internal and external causes mostly impact the CT images. Therefore, a hybrid filter using a mixture of Gaussian and median is applied in this research to minimize noise in CT pancreatic images. The Gaussian filter is applied to minimize the noise in the CT scans as well as the residual variations of geographical intensities. The Gaussian filter is utilized to replace the noisy pixels in the images with the Gaussian-distributed average value of the surrounding pixels. The median filter, on the other hand, may effectively remove spiky noises while maintaining the image's crisp edges and will also restore each pixel's grey level. In order to segment the images of pancreatic cancer, the noise-reduced images are employed in the ALO-CNN-GRU model.

The equation for the Gaussian filter is:

$$G(r) = \frac{1}{\sqrt{2\pi\sigma^2}} e^{-\frac{r^2}{2\pi\sigma^2}} \quad (1)$$

Where σ is the standard deviation of the distribution. The distribution's mean is considered to be zero.

The equation for the median filter is:

$$\hat{g}(m, n) = \text{median}_{(s,t) \in T_{mn}} \{f(s, t)\} \quad (2)$$

Here $f(s, t)$ residual pixel following removal.

The improved equation for the pre-processing of CT images is:

$$\hat{g}(m, n) = \text{median}_{(s,t) \in T_{mn}} \{G(r)\} \quad (3)$$

Here r is the pixel dimension of every image. Every image is denoted by m .

C. Segmentation

The segmentation process is primarily employed to segment the affected region in the visualizations of CT images. The performance of image processing depends on how well the segmentation process works. Image segmentation is widely used to pinpoint an image's influenced areas as well as the constraints imposed by its curves and lines. The process of image segmentation divides each collection of pixels in the images into its own group of labels. In medical image processing, image segmentation's primary goal is to locate the cancer-affected regions and provide sufficient information for further identification. The identification of morphological characters and the detection of pancreatic cancer typically involve pancreas segmentation. Nevertheless, due to the significant anatomical heterogeneity of the pancreas, precise segmentation remains difficult. For this purpose, we segment the pancreas utilizing Antlion Optimization (ALO).

1) *Antlion optimization:* The Ant Lion (called Antlion) optimization algorithm imitates an antlion's natural hunting strategy. While antlions primarily hunt as larvae, the adult period is used for reproducing. A larval antlion moves in a circle while ejecting sand with its muscular jaws to create a cone-shaped opening in the sand. Following the construction of the traps, the larvae conceal underneath the base of the cone and waits for insect species ants—to enter the hole and become entangled. When the antlion discovers that there is prey in the trap, it tries to catch its victim. Although they try to get away from the trap, insects are often not immediately caught. In this case, antlions cunningly throw grains along the edge of the opening to assist the prey in slipping towards the bottom of the pit. A prey that is captured in the jaws is dragged under the ground and eaten. Antlions discard the remaining prey outside of the hole after eating it and prepare the pit for the subsequent hunt. Another noteworthy aspect of antlions' way of life is the relationship between the dimensions of the traps, one's personal level of hunger, and the form of the moon.

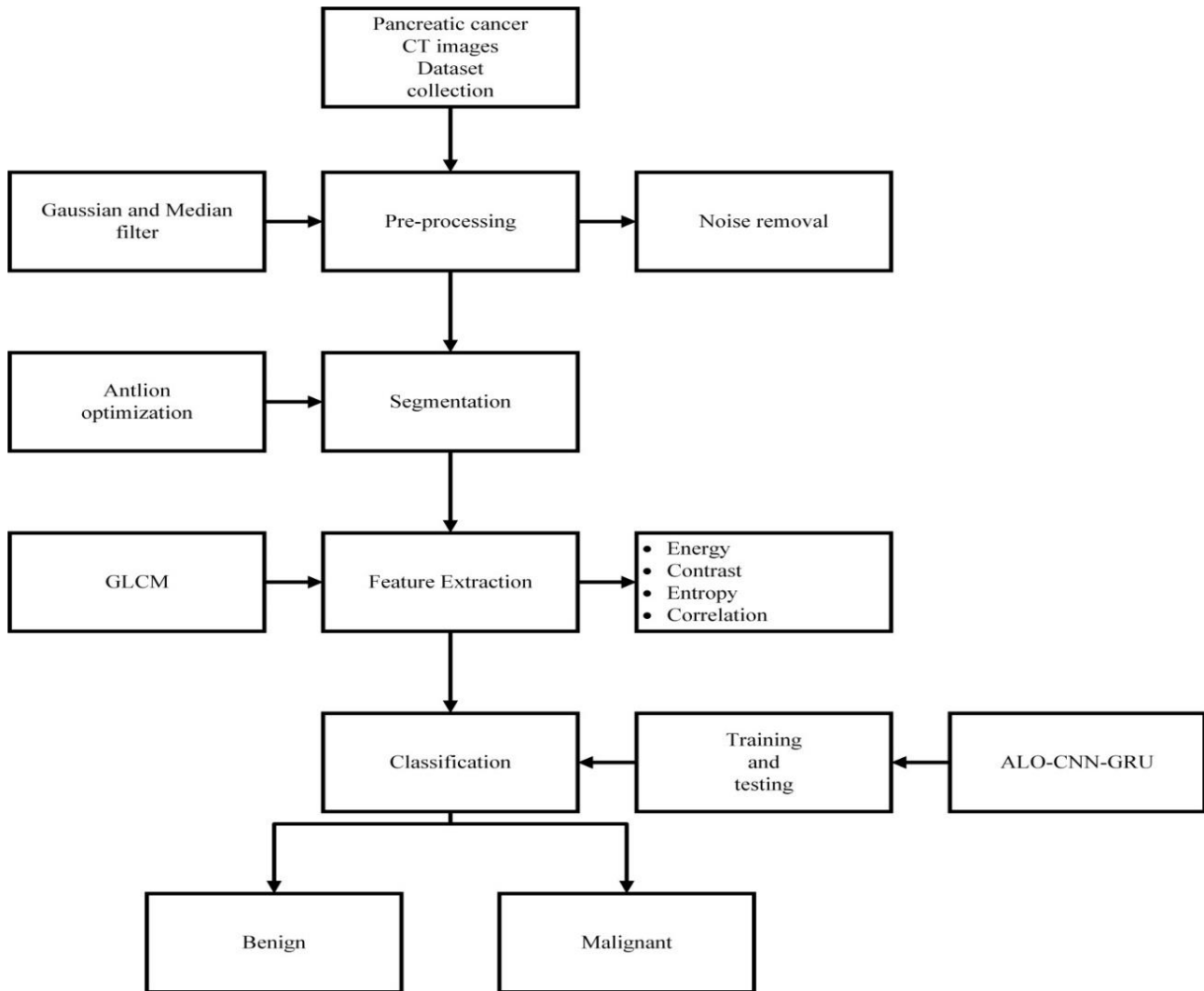


Fig. 1. Proposed method's framework.

2) *ALO algorithm operators*: The ALO algorithm simulates ant behaviour in nature, including how they create trap and goes on the hunts. Ants taking lengthy walks at random. The ant moves arbitrarily throughout the search area in accordance with equation (4).

$$X_i^t = \frac{(x_i^t - b_i) \times (h_i - G_i^t)}{(h_i - b_i)} + G_i \quad (4)$$

where b_i is the random walk's i -th variable's minimum value, G_i^t is the i -th variable's minimal value at the t -th iteration, and h_i reflects the highest value for variable i at iteration t . The ant random walk is normalized to the maximum or minimum values of the search area if it occurs outside the search area.

3) *Trapping in antlions pits*: The antlion traps have an impact on the ants' random travels. It is demonstrated that a variety of variables govern the ants' random travels (g , h). Where g is the lowest consistent factor for i -th ant and h is the highest consistent factor for i -th ant.

$$g_i^t = Antlion_j^t + G^t$$

$$h_i^t = Antlion_j^t + h^t \quad (5)$$

4) *Building trap*: The ability of an antlion to hunt was modelled using a roulette wheel. The person operating the roulette wheel chooses the antlion based on its fitness because only one antlion is allowed to capture every ant. The likelihood of catching ants increases with an antlion's fitness.

5) *Ants moving toward the antlion*: The antlion begins to spray sand outward from the center of the trap once it understands there's an ant in the conic hole. Flexible reduction of the ant's random journey range is calculated as follows:

$$g^t = \frac{g^t}{I}$$

$$h^t = \frac{h^t}{I} \quad (6)$$

where g^t the smallest of all the variable at the t -th iterations, and h^t shows the vectors that contains the most variable at the t -th iterations.

6) *Prey capture and trap construction*: Subsequently, the antlion captures the ant and consumes its body when the ant

grows stronger than it. To improve its chances of a new hunt, the antlion changes its location to match that of the hunted ant. The suggested equation is shown below.

$$Antlion_j^t = Ant_i^t, \text{ if } f(Ant_i^t) > f(Antlion_j^t) \quad (7)$$

The antlion known as the Elite-Antlion is the one that consistently provides the best answer across all iteration and searches domains. Every iteration compares the elite-antlion to the antlion only with best fitness. By using the ant's randomness algorithm throughout the roulette wheel (R_B^t) and the unplanned excursion of Elite-Antlion (R_P^t), the elite-antlion strategy affects how the ants wander randomly around the antlion.

$$Ant_i^t = \frac{R_B^t + R_P^t}{2} \quad (8)$$

The complete flow chart of the working process is given below in Fig. 2.

Algorithm 1: ALO-CNN-GRU mechanism

Input: Computerized Tomography Images

Output: Benign, malignant

Import input CT image data

Let I be the input data that is taken for analysis

$$I = \{I_1, I_2, I_3 \dots\}$$

Pre-processing of images //Gaussian
and median
filter
Segmentation of images //Antlion
Optimization

Create a population of n ants and n antlions at random
starting sites

Determine each ant's and antlion's fitness

Locate the elite antlion;

$t=0$

While ($t \leq T$)

Foreach ant_i do

Use the roulette wheel to choose an antlion

Entice ants to approach the antlion

Construct a random walk to ant_i and normalize

End

Compute each ant's level of fitness

To become fitter, swap an antlion for the equivalent ant

If an antlion gets more fit than the elite, upgrade the elite
end if

Feature extraction //GLCM
Classification //CNN-GRU
classifier

Classifying as benign, malignant
end if
end while

D. Feature Extraction

The feature extraction process entails transforming unstructured data into numerical qualities that may be used to

protect the data included in the original set of information. These characteristics, which are obtained from every one of the CT images that were taken, represent how each patient interprets CT scans individually. During testing, the images' dimensionality is enhanced. However, in order to identify pancreatic cancer, the dimensionality of the images must be decreased. To fix this problem, the feature extraction process was being used.

In the feature extraction, the Gray Level Co-occurrence Matrix (GLCM) is utilized. By calculating the pairings of pixels with specific values, it may calculate the structure of the images. The GLCM analyses the image's grayscale to determine the pixels' brightness. Energy, Correlation, homogeneity, entropy, contrast, and other properties of the second-order representations are evaluated for the purpose of deleting the statistical texture characteristic.

1) *Energy*: Energy is described as the insertion of a square in images when the concentration levels are unequal, and the grey levels are often greater. Eq. (9) is used to determine the energy of the input data.

$$E = \sum_j \sum_k \{V(j, k)\}^2 \quad (9)$$

where an image is indicated as V and grey level squares are denoted as (j, k) .

2) *Contrast*: When an image's local contrast is evaluated, attributes are used, and when the concentration is even, a low value is calculated. The original images contrast and total number of grey levels are projected in eqn. (10)

$$C = \sum_{m=0}^{Pq} m \{ \sum_{j=1}^{Pq} \sum_{k=1}^{Pq} V(j, k) \} \quad (10)$$

where P denote the grey level of the images, V denotes the images, and (j, k) denotes the grey level square of the images.

3) *Correlation*: The correlation characteristics could be utilized to account for both the linear dependency of the grey levels on the pixels and the numerical correlations between the variables. In eq. (11), the qualities are revealed.

$$C = \frac{\sum_j \sum_k (j,k) V(j,k) - \mu_m \mu_n}{\sigma_m \sigma_n} \quad (11)$$

The mean and standard deviation values, in the images, are $\mu_m, \mu_n, \sigma_m, \sigma_n$ which are defined as row and column, respectively.

4) *Entropy*: The expected significant amount of the unpredictability of the distribution of the grey level, which is indicated in eq. (12), is referred to as entropy.

$$En = - \sum_j \sum_k V(j, k) \log(V(j, k)) \quad (12)$$

E. Classification using CNN and GRU

1) *Convolutional neural network*: Utilizing many CNN front layers, which are used to uncover patterns in images, convolutional neural networks are able to recognize lines and corners.

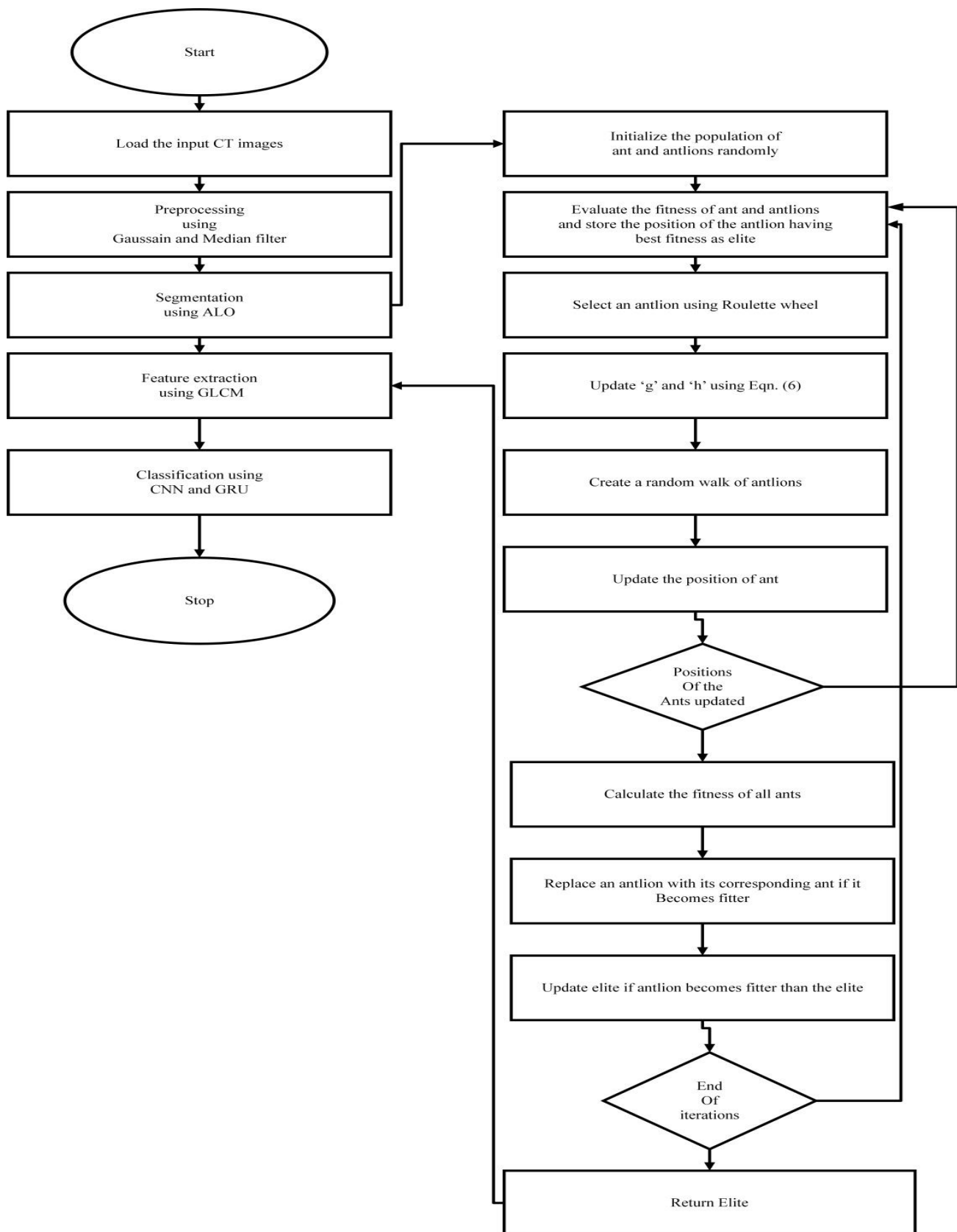


Fig. 2. ALO-CNN-GRU technique flow chart.

However, when they get farther into the neural network, they may transfer these patterns there and attempt to find more distinguishing properties. For extracting image features, the CNN model is incredibly effective. Furthermore, the suggested CNNs model, according to the researchers, successfully distinguishes pancreatic CT scans. The pooling, convolutional layer (CLs), and fully connected layers make up the CNN's three major layers (FCs). Calculating the results of neurons connected to local sites is the responsibility of the CLs. By taking into account the region's and weights' dot product, it is decided. The common filters in the instance of the input images are made up of small area pixels. These filters can examine the images by swiping a window over them while automatically regulating any recurring patterns that show up in any image location. The stride is the separation in a series of filters. In the event that the initial parameter set is less than any one of the filter dimensions, they expand the convolution to incorporate screens that overlap. Each image's equation from the training set is given in Eq. (13)

$$p(c, q) = \frac{o(c,q)-\mu}{\sigma} \quad (13)$$

a) *Convolutional layer*: The convolutional layer uses every layer to examine every image's complexity after collecting a range of input images. It is connected directly to the characteristics needed in the given image. It is expressed in Eq. (14)

$$f_i^n = x(\sum_{j \in N_i} f_j^{n-1} * p_{ji}^n + t_i^n) \quad (14)$$

N_i – It stands for an input choice. The output is a bias that is additive. The kernel used for the map i, which if the map t and map s both sums over map i.

b) *Max pooling layer*: This layer is included in the down sampling layer to minimize fitting and the quantity of the neurons utilized. In addition to controlling overfitting, the pooling layer minimizes the size of the feature map, number of parameters, pace of computation, and the training time. It is calculated by using eqn. (15)

$$x_{mab} = \max_{(c,d) \in f_{ncd}} \quad (15)$$

Map, f_{ncd} is the element as (c, d) within the pooling region pts which represents a local neighbourhood around the place (t, s).

c) *Fully connected layer*: Fully Connected Layer has been employed for the representation classification context. Convolutional layers are put first, then FC layers. The output and input illustrations are mapped using the Fully Connected layer. The last layers of the network are completely coupled layers. The output of the max pooling layer serves as the input for the fully connected layer.

d) *Softmax layer*: The Softmax layer converts the values into a standardized proportion distribution. The classifier receives the output as an input. The Softmax classifier is a standard contribution classifier that applies the Softmax layer's structure to pancreatic cancer nodules. It is shown in Eq. (16)

$$\sigma(\vec{X})_a = \frac{e^{x_a}}{\sum_{i=1}^n e^{x_i}} \quad (16)$$

2) *Gated recurrent unit network*: In order to solve the gradient vanishing problem, the GRU model was most frequently used in recurrent neural networks (RNN). GRU is more effective than LSTM since it has an internal cell state and three primary gates. The data is kept in a secure location within the GRU. The update gate offers both past and forward information, whereas the reset gate offers previous knowledge. The needed data from the former condition of the system is preserved and kept by the present memory gate using the reset gate. The input modulation gate allows for the introduction of nonlinearity while simultaneously giving the input zero-mean properties. The mathematical formulation of the basic GRU of rest and updated gates is, as defined by the following,

$$A_t = \sigma(Y_t \cdot Z_{ya} + F_{t-1} \cdot Z_{ha} + d_a) \quad (17)$$

$$B_t = \sigma(Y_t \cdot Z_{yb} + F_{t-1} \cdot Z_{hb} + d_b) \quad (18)$$

where Z_{ya} and Z_{yb} present weight parameters, while the d_a, d_b are biased. Fig. 3 represents the fundamental design of the GRU model.

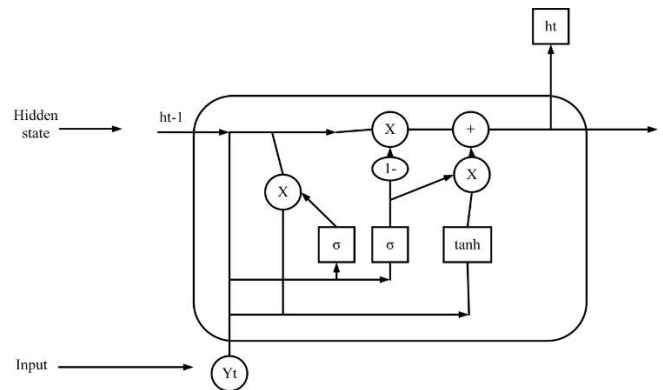


Fig. 3. The fundamental design of the GRU model.

3) *Combined CNN-GRU*: Four convolution layer (CL) layers, three max-pooling layers, and three fully linked layers made up the CNN-GRU model (FC). The activation function was included since it might not stimulate every neuron at once, which improves performance and speeds up learning. The raw image data were initially provided with the dimensions in CLs. Features must be extracted for the CNN-GRU model by going through Convolutional Layers. To reduce the nonlinearity dimension, ReLUs were combined with Convolutional Layers. The parameter for the training dataset is likewise decreased by the pooling layer. After the pooling layer, the training variables were transferred over from the hidden layer to avoid overfitting issues in the system. Fig. 4 represents the overall structure of the CNN-GRU model.

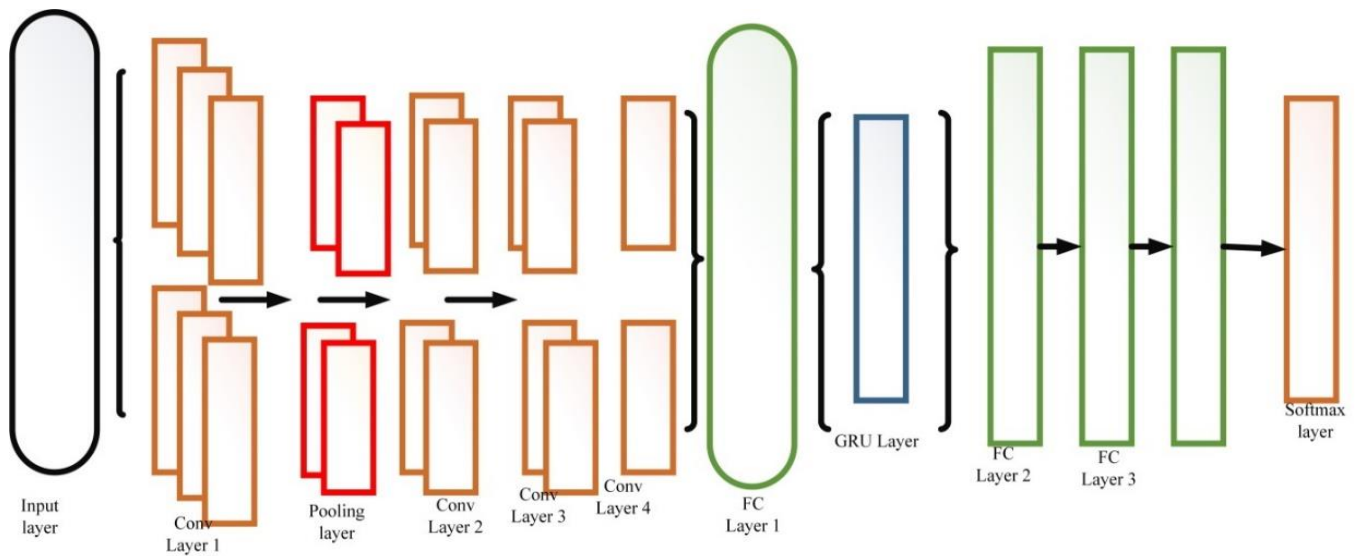


Fig. 4. Overall structure of the CNN-GRU model.

IV. RESULTS AND DISCUSSION

A dataset of images from computerized tomography is used to evaluate the suggested strategy. The 1782 CT images were pre-processed utilizing a hybrid Gaussian and median filter. CT image pre-processing is essential for enhancing the image's visual appeal before additional processing. The images in the collection often contain noise; the noise is removed by pre-processing. After that, the segmentation process is completed using the Antlion optimization method. The areas of pancreatic cancer are identified and separated throughout this procedure. The Gray Level Co-occurrence Matrix then does the feature extraction. The combined CNN-GRU performs the classification after that. The effectiveness of the offered technique is assessed using performance indicators such as Recall, Accuracy, F-measure, and Precision.

A. Accuracy

The model of the system accuracy is a measure of how precisely it functions across all classes. Generally, it is the statement that all observations are accurately expected observations. Accuracy is expressed in Eq. (19),

$$Accuracy = \frac{T_{pos} + T_{neg}}{T_{pos} + T_{neg} + F_{pos} + F_{neg}} \quad (19)$$

TABLE I. COMPARISON OF ACCURACY

Methods	Accuracy (%)
IDLDMS	99.35
Multi resolution CNN	89.67
CE-ConvLSTM	73.6
ODL-PTNTC	98.82
Proposed ALO-CNN-GRU	99.92

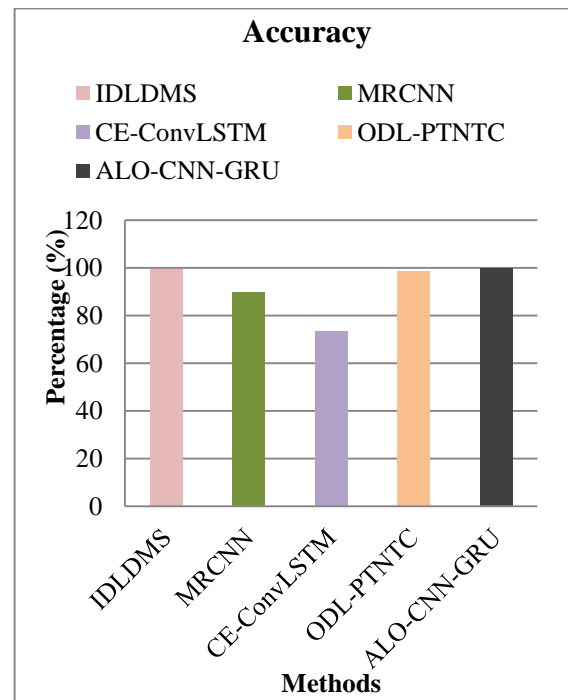


Fig. 5. Comparison of accuracy.

When compared to the current Pancreatic cancer segmentation and classification techniques like IDLDMS, MRCNN, CE-ConvLSTM, ODL-PTNTC, which are shown in Table I, the projected methodology ALO-CNN-GRU obtains superior accuracy. The accuracy of ALO-CNN-GRU and other approaches is compared in Fig. 5.

B. Precision

Precision is determined by counting the precise positive ratings that differ from the total positive evaluations. By using eqn. (20), it is possible to determine the accurate identification of cancer nodules in the afflicted area.

$$P = \frac{T_{pos}}{T_{pos} + F_{pos}} \quad (20)$$

TABLE II. COMPARISON OF PRECISION

Methods	Precision (%)
IDLDMS	99.35
Multi resolution CNN	91.37
CE-ConvLSTM	81.3
ODL-PTNTC	98.73
Proposed ALO-CNN-GRU	99.64
AAT	95.2
LLE	96.55

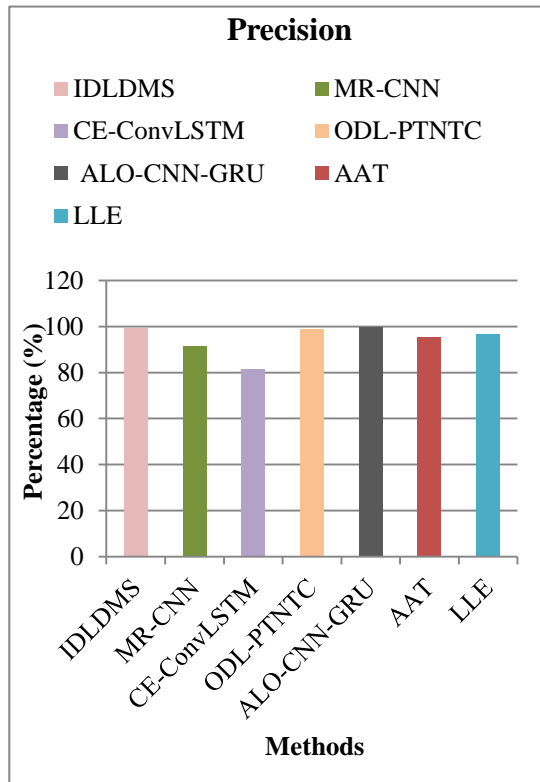


Fig. 6. Comparison of precision.

The precision comparison between ALO-CNN-GRU and other methods is shown in Fig. 6. Table II shows that the proposed Antlion Optimization-Convolutional Neural Network-Gated Recurrent Unit strategy outperforms previous pancreatic cancer segmentation and classification methods including IDLDMS, MR-CNN, CE-ConvLSTM, ODL-PTNTC, AAT, and LLE with a greater precision of 99.64%.

C. Recall

The recall is the ratio of the total amount of positive sample to the number of actual positives that were accurately

classified as positives. It displays the percentage of prediction about the identification of tumor nodules indicated by Eq. (21) were correct.

$$R = \frac{T_{pos}}{T_{pos} + F_{neg}} \quad (21)$$

TABLE III. COMPARISON OF RECALL

Methods	Recall (%)
IDLDMS	98.84
Multi resolution CNN	93.63
CE-ConvLSTM	65.9
ODL-PTNTC	98.73
Proposed ALO-CNN-GRU	99.53
AAT	95.8

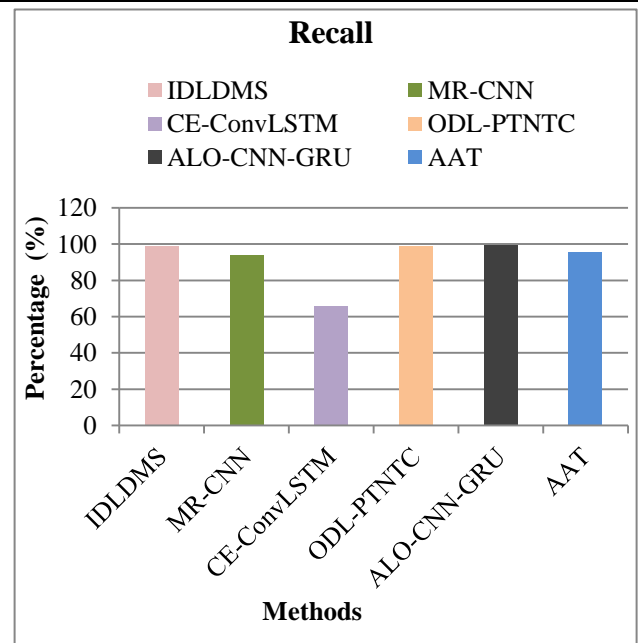


Fig. 7. Comparison of recall.

The suggested methodology ALO-CNN-GRU greatly improves recall comparing to the current Pancreatic cancer segmentation and classification techniques such IDLDMS, MR-CNN, CE-ConvLSTM, ODL-PTNTC, and AAT, as shown in Table III. Fig. 7 displays the recall comparison between ALO-CNN-GRU and other methods.

D. F1-Score

Recall and precision are combined in the F1-Score computation. The F1-Score is computed using recall and precision that is represented in Eq. (22),

$$F1 - score = \frac{2 \times precision \times recall}{precision + recall} \quad (22)$$

TABLE IV. COMPARISON OF F1-SCORE

Methods	F1-Score (%)
IDLDMS	99.48
Multi resolution CNN	84.97
CE-ConvLSTM	70.5
ODL-PTNTC	98.82
Proposed ALO-CNN-GRU	99.72

Fig. 8 illustrates a comparison of the ALO-CNN-GRU and other methodologies' F1-Scores. Table IV demonstrates that the proposed methodology, Antlion Optimization-Convolutional Neural Network-Gated Recurrent Unit technique, achieves a superior F1-Score in comparison to the current pancreatic cancer segmentation and classification approaches, such as IDLDMS, MR-CNN, CE-ConvLSTM, and ODL-PTNTC.

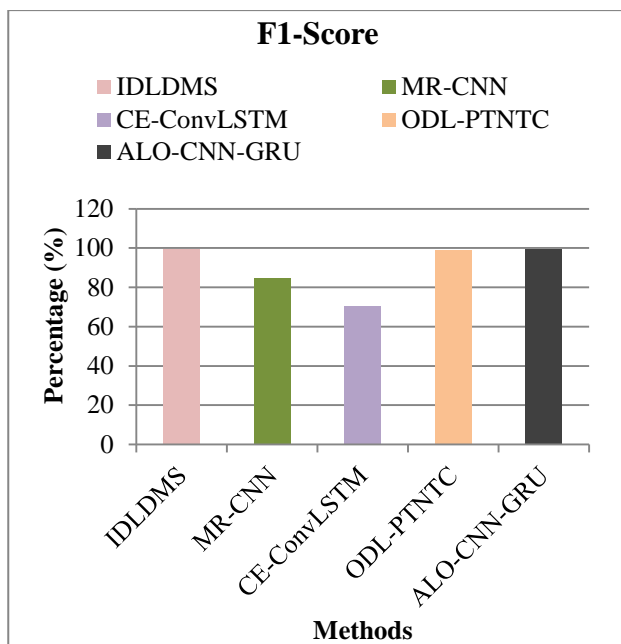


Fig. 8. Comparison of F1-score.

V. CONCLUSION

An essential part of the human body, the pancreas performs both internal and exterior secretion duties and is prone to a number of illnesses. Pancreatic malignancies, which are deadly in nature, currently have very poor prognoses. Computerized pancreatic cancer segmentation and classification utilizing a computer-aided diagnostic model is needed to monitor, identify, and categorize the incidence of cancer. Accurate image interpretation can be provided throughout deep learning algorithms for therapeutic application. To achieve this goal, the study created an ALO-CNN-GRU model for CT images and deep learning-based pancreatic tumor segmentation and classification. To remove noise from the acquired dataset, the images go through pre-processing. For the pre-processing, a hybrid Gaussian and median filter is being used. The segmentation is performed

using the Antlion optimization algorithm to determine the impacted pancreatic region. Next, the classifiers of the Convolutional neural network and Gated Recurrent Unit networks are used to categorize pancreatic cancer as benign and malignant. We examined recall, accuracy, precision, and F1-score as performance indicators. Better performance metrics are produced by the suggested ALO-CNN-GRU technique. The experimental results back up the claim that the suggested strategy works better than approaches already in use. In order to accurately detect and categorize the pancreatic cancer locations, future versions of the methods will employ LSTM with additional deep learning mechanisms and combine sophisticated optimization with classification algorithms.

ACKNOWLEDGMENT

The authors extend their appreciation to the Deanship of Scientific Research at Saudi Electronic University for logistic support for this work through the 2nd Interdisciplinary Scientific Research Hackathon, project no. (SRH005T1).

REFERENCES

- [1] S.-L. Liu et al., "Establishment and application of an artificial intelligence diagnosis system for pancreatic cancer with a faster region-based convolutional neural network," *Chin. Med. J. (Engl.)*, vol. 132, no. 23, pp. 2795–2803, Dec. 2019, doi: 10.1097/CM9.0000000000000544.
- [2] M. Reyngold, P. Parikh, and C. H. Crane, "Ablative radiation therapy for locally advanced pancreatic cancer: techniques and results," *Radiat. Oncol.*, vol. 14, no. 1, p. 95, Dec. 2019, doi: 10.1186/s13014-019-1309-x.
- [3] K.-L. Liu et al., "Deep learning to distinguish pancreatic cancer tissue from non-cancerous pancreatic tissue: a retrospective study with cross-racial external validation," *Lancet Digit. Health*, vol. 2, no. 6, pp. e303–e313, Jun. 2020, doi: 10.1016/S2589-7500(20)30078-9.
- [4] I. Joo et al., "Preoperative CT Classification of the Resectability of Pancreatic Cancer: Interobserver Agreement," *Radiology*, vol. 293, no. 2, pp. 343–349, Nov. 2019, doi: 10.1148/radiol.2019190422.
- [5] Y. Iwatate et al., "Radiogenomics for predicting p53 status, PD-L1 expression, and prognosis with machine learning in pancreatic cancer," *Br. J. Cancer*, vol. 123, no. 8, pp. 1253–1261, Oct. 2020, doi: 10.1038/s41416-020-0997-1.
- [6] H. Nasief et al., "A machine learning based delta-radiomics process for early prediction of treatment response of pancreatic cancer," *Npj Precis. Oncol.*, vol. 3, no. 1, p. 25, Dec. 2019, doi: 10.1038/s41698-019-0096-z.
- [7] Y. Toyama, M. Hotta, F. Motoi, K. Takanami, R. Minamimoto, and K. Takase, "Prognostic value of FDG-PET radiomics with machine learning in pancreatic cancer," *Sci. Rep.*, vol. 10, no. 1, p. 17024, Oct. 2020, doi: 10.1038/s41598-020-73237-3.
- [8] O. M. Griffin, S. N. Duggan, R. Ryan, R. McDermott, J. Geoghegan, and K. C. Conlon, "Characterising the impact of body composition change during neoadjuvant chemotherapy for pancreatic cancer," *Pancreatology*, vol. 19, no. 6, pp. 850–857, Sep. 2019, doi: 10.1016/j.pan.2019.07.039.
- [9] S. Srisajakul, P. Prapaisilp, and S. Bangchokdee, "CT and MR features that can help to differentiate between focal chronic pancreatitis and pancreatic cancer," *Radiol. Med. (Torino)*, vol. 125, no. 4, pp. 356–364, Apr. 2020, doi: 10.1007/s11547-019-01132-7.
- [10] A. D. Singhi, E. J. Koay, S. T. Chari, and A. Maitra, "Early Detection of Pancreatic Cancer: Opportunities and Challenges," *Gastroenterology*, vol. 156, no. 7, pp. 2024–2040, May 2019, doi: 10.1053/j.gastro.2019.01.259.
- [11] L. Boldrini, D. Cusumano, F. Cellini, L. Azario, G. C. Mattiucci, and V. Valentini, "Online adaptive magnetic resonance guided radiotherapy for pancreatic cancer: state of the art, pearls and pitfalls," *Radiat. Oncol.*, vol. 14, no. 1, p. 71, Dec. 2019, doi: 10.1186/s13014-019-1275-3.

- [12] S. Rudra et al., "Using adaptive magnetic resonance image-guided radiation therapy for treatment of inoperable pancreatic cancer," *Cancer Med.*, vol. 8, no. 5, pp. 2123–2132, 2019, doi: 10.1002/cam4.2100.
- [13] S.-L. Liu et al., "Establishment and application of an artificial intelligence diagnosis system for pancreatic cancer with a faster region-based convolutional neural network," *Chin. Med. J. (Engl.)*, vol. 132, no. 23, pp. 2795–2803, Dec. 2019, doi: 10.1097/CM9.0000000000000544.
- [14] J. Li, L. Qi, Q. Chen, Y.-D. Zhang, and X. Qian, "A dual meta-learning framework based on idle data for enhancing segmentation of pancreatic cancer," *Med. Image Anal.*, vol. 78, p. 102342, May 2022, doi: 10.1016/j.media.2021.102342.
- [15] T. Vaiyapuri et al., "Intelligent Deep-Learning-Enabled Decision-Making Medical System for Pancreatic Tumor Classification on CT Images," *Healthcare*, vol. 10, no. 4, Art. No. 4, Apr. 2022, doi: 10.3390/healthcare10040677.
- [16] Y. Xia et al., "Effective Pancreatic Cancer Screening on Non-contrast CT Scans via Anatomy-Aware Transformers," in *Medical Image Computing and Computer Assisted Intervention – MICCAI 2021*, vol. 12905, M. de Bruijne, P. C. Cattin, S. Cotin, N. Padoy, S. Speidel, Y. Zheng, and C. Essert, Eds. Cham: Springer International Publishing, 2021, pp. 259–269. doi: 10.1007/978-3-030-87240-3_25.
- [17] X. Yang, Y. Chen, X. Yue, C. Ma, and P. Yang, "Local linear embedding based interpolation neural network in pancreatic tumor segmentation," *Appl. Intell.*, vol. 52, no. 8, pp. 8746–8756, Jun. 2022, doi: 10.1007/s10489-021-02847-9.
- [18] V. Asadpour, R. A. Parker, P. R. Mayock, S. E. Sampson, W. Chen, and B. Wu, "Pancreatic cancer tumor analysis in CT images using patch-based multi-resolution convolutional neural network," *Biomed. Signal Process. Control*, vol. 68, p. 102652, Jul. 2021, doi: 10.1016/j.bspc.2021.102652.
- [19] J. Yao, Y. Shi, L. Lu, J. Xiao, and L. Zhang, "DeepPrognosis: Preoperative Prediction of Pancreatic Cancer Survival and Surgical Margin via Contrast-Enhanced CT Imaging." arXiv, Aug. 26, 2020. Accessed: Dec. 13, 2022. [Online]. Available: <http://arxiv.org/abs/2008.11853>
- [20] M. M. Althobaiti, A. Almulihi, A. A. Ashour, R. F. Mansour, and D. Gupta, "Design of Optimal Deep Learning-Based Pancreatic Tumor and Nontumor Classification Model Using Computed Tomography Scans," *J. Healthc. Eng.*, vol. 2022, pp. 1–15, Jan. 2022, doi: 10.1155/2022/2872461.